



Investigation of Dielectric Properties of Ni/n-TiO₂/p-Si/Al Heterojunction in Wide Range of Temperature and Voltage

A. Kumar^a, A. Kumar^{*b}, K. K. Sharma^a

^a Department of Physics and Photonics Science, National Institute of Technology, Hamirpur, India

^b Department of Physics, Government College Sujapur Tihra, India

PAPER INFO

Paper history:

Received 23 August 2021

Received in revised form 31 December 2021

Accepted 11 January 2022

Keywords:

Dielectric Constant

Electric Moduli

Conductivity

Interface States

ABSTRACT

In the present study we have investigated the dielectric properties such as dielectric constant (ϵ'), dielectric loss (ϵ''), real part of electrical modulus (M'), imaginary part of electric modulus (M'') and AC electrical conductivity, (σ_{ac}) in wide range of applied voltage, temperature and frequency for Ni/n-TiO₂/p-Si/Al heterojunction. A nanocrystalline TiO₂ layer was grown on p-type boron doped silicon in oxygen-controlled environment using optimized KrF excimer laser. Ohmic contact of pure nickel and aluminum metals was made on TiO₂ and silicon respectively, with thermal coating system. The characteristics obtained with the help of conductance-voltage and capacitance-voltage measurements also known as impedance/admittance spectroscopy. The studied parameters are found to be very sensitive to frequency, temperature and voltage. The restructuring and reordering of interface state density due to temperature variations and interfacial polarizations due to frequency variations collectively result the observed changes in the ϵ' and ϵ'' . With an increase in frequency AC conductivity and electrical modulus also increases. The relaxation mechanism can be observed in the complex electrical modulus analysis. The thermally activated conduction process was indicated by the frequency dependent AC conductivity at different temperatures. Using power law, the AC conductivity was analyzed and found to increase with temperature, applied voltage.

doi: 10.5829/ije.2022.35.04a.09

1. INTRODUCTION

In semiconductor technology the metal semiconductor heterojunctions are well known basic devices which are used in various electronic circuits. These devices are very significant for the electronic industry [1-3] because of their technological applications as rectifiers, inverters, polarity protection solar cells, photodetectors etc. The stability, reliability and performance of these devices are dominantly influenced by the characteristics prevailing at the interface [4]. The density of interface states at the interface of heterojunction and also the interfacial layer thickness dominantly impacts the dielectric and electrical parameters of these devices [5-7]. The interface capacitance also known as excess capacitance is strongly dependent on frequency and voltage which in turn strongly affect the admittance spectroscopy of the

devices [5-8]. The frequency response of ϵ' and ϵ'' shows strong dispersion at low frequencies [9-10]. The presence of metal oxide thin films significantly changes the dielectric and electric behavior of the heterojunction devices [11-15]. Moreover, there is formation of large number of defects and impurities at the semiconductor surface as a result of periodic interruption of lattice structure. These physical processes result the large number of energy levels associated with interface states well within the energy band gap of the semiconductor which are strongly influenced by applied frequency, temperature and voltage. So, it is obvious that the existence of the localized interface states greatly alters the functioning and characteristics of the device from the ideal case by modifying the electric and dielectric parameters of the heterojunction devices [16-21]. These dependencies occur because the temperature variations of

*Corresponding Author Email: puri_nir@yahoo.com (A. Kumar)

the device lead to the interface states readjustments and sharing of applied bias between depletion layer, interfacial layer and series resistance [20-21]. The $C-V$ and $G/\omega-V$ analysis in the forward as well as in reverse direction only at small frequency range cannot supply the comprehensive information about the electrical and dielectric properties of the device. Whereas, wide range frequency measurements can supply complete information about the dielectric properties along with the transport mechanism of the devices [22-25]. The electrode polarization due to the accumulation of charges hides the relaxation processes and the complete analysis of the device parameters becomes difficult. In these cases, the complex electrical modulus is a powerful tool for understanding bulk relaxation processes because it minimizes conductivity and permittivity variations in the low frequency regions [26-27].

The modified behavior observed in electrical and dielectric characteristics of the heterojunction diodes is generally due to the effect of interfacial layer properties [28-30]. In general, the $C-V$ and $G/\omega-V$ characteristics of these devices in an ideal situation are independent of frequency [31-32]. But the idealized situations are often disturbed by the interfacial layer separating the metal semiconductor junction and also by interface states at the interface of thin oxide layer and the semiconductor [31-33]. The characteristics of the heterojunction diodes can be deliberately modified when a suitable thin layer separate the metal from semiconductor component [34-36].

Since the electronic device applications are significantly influenced by the dielectric properties of the heterojunction, so in the present study we have made the detailed analysis of the dielectric properties namely, dielectric constant (ϵ'), dielectric loss (ϵ''), real and imaginary electric modulus (M', M'') and AC electrical conductivity (σ_{ac}) of the heterojunction Ni/n-TiO₂/p-Si/Al through admittance/impedance spectroscopic techniques which require the $C-V$ and $G/\omega-V$ measurements in wide temperature and voltage ranges at different frequencies.

2. EXPERIMENTAL PROCEDURE

First, aluminum metal was deposited on the back side of p-type silicon wafer with (100) surface orientation under 3×10^{-6} mbar vacuum to form the ohmic contacts followed by annealing for 1 h at 300 °C to achieve best ohmic performance. Then TiO₂ thin films were grown on using pulsed laser ablation technique to fabricate Ni/n-TiO₂/p-Si/Al heterojunction diode. The sintered pallets of TiO₂ at 1000 °C for 12 h were used for deposition of thin films. To ablate the TiO₂ target KrF (248 nm) COHERENT COMPLEX PRO 205 F laser was used with

repetition rate of 10 Hz at energy of 300 mJ. Eventually, nickel metal was thermally evaporated through masks with circular holes of 1 mm diameter from the tungsten filament into the TiO₂ film to form metal contacts. Ni/TiO₂ and p-Si/Al interfaces are ohmic in nature. Wayne Kerr 6520A, precision impedance analyzer was employed to study the $C-V$ and $G/\omega-V$ measurements.

3. RESULTS AND DISCUSSIONS

3.1. Dielectric Studies at Different Voltages The complex permittivity can be expressed through the following relation [37]:

$$\epsilon^* = \epsilon' - i\epsilon'' = \frac{C}{C_0} - i \frac{G}{\omega C_0} \quad (1)$$

The values of ϵ' and ϵ'' can be expressed using Equation (1) as:

$$\epsilon' = \frac{C}{C_0} \quad (2)$$

$$\epsilon'' = \frac{G}{\omega C_0} \quad (3)$$

ϵ^* is the complex dielectric constant, $C_0 = \frac{\epsilon_0 A}{d}$, is the capacitance of capacitor without any dielectric, A is the diode area, ϵ_0 is the permittivity of free space and d is the thickness of interlayer, i is the imaginary root of $\sqrt{-1}$, ω is the angular frequency.

The variations of ϵ' and ϵ'' with logarithmic frequency $\ln(\omega)$ for the Ni/n-TiO₂/p-Si/Al heterojunction have been evaluated by using equations (2) and (3) at different applied voltages. The charge reordering and restructuring due to the external bias at n-TiO₂/p-Si interface and interface polarization usually produce the change in conductivity of the device. The dielectric characteristics as well as interface properties dominantly affect the electric parameters of the device since the interface states respond differently in the high and low frequency regimes. So the quantities, ϵ' and ϵ'' are plotted with frequency in Figures 1 and 2, respectively, for various forward bias voltages and then comprehensively analyzed in the following.

The experimental values of ϵ' and ϵ'' as a function of frequency at selected applied voltages from 0.2 V to 2.0 V, as shown in Figs. 1 and 2 are found to be strongly dependent on frequency as well as applied voltage. Moreover, at low and intermediate frequency range the variations become considerably high while they become almost frequency independent in the high frequency regimes. The swingeing decrease in the values of ϵ' and

ϵ'' with increase in frequency shows the shortage of time available for interfacial dipoles to align themselves with the direction of external alternating electric field [38-39]. Due to the insufficient time available, the dipoles are unable to orient themselves with the field at very high frequency and this results the decrease in the dielectric constant values [40]. The displacement of charges from the traps or equilibrium states occur as a result of the polarization of dielectric or polymeric material at low and intermediate frequencies under the effect of external field. So, it is obvious that the relaxation time plays a dominant role in changing of dielectric properties with the frequency of applied field. In this study it is revealed that the interfacial as well as dipole polarization can easily take place at low and intermediate frequencies. Moreover, the charges in the traps follow the field at low frequencies thereby increasing the dielectric constant. However, the inability of interface states in following the high frequency signal leads to the saturation of dielectric constant. At this stage interface states do not contribute towards admittance spectroscopy hence ϵ' and ϵ'' values become independent of the frequency of the field since there is the absence of any mechanism which can produce interface polarization. The charges located at the surface states or interface traps which are between the semiconductor and the interfacial layer greatly impact the dielectric and electric properties of the devices because the release of this charge on the application of appropriate external AC voltage produce a charge effect in these devices [4, 41]. The frequency dependent dispersion observed in dielectric constant as well as in the dielectric loss is mainly due to the Maxwell–Wagner process [34] and space charge polarization [35]. The Maxwell–Wagner process is associated with the relaxation time that deals with the surface charges that remain uncompensated at interface inside the capacitors [36].

3. 2. Dielectric Studies at Different Temperatures

Figure 3 depicts the changes in dielectric constant with the logarithmic angular frequency of the applied AC signal applied at different temperatures. Here it was

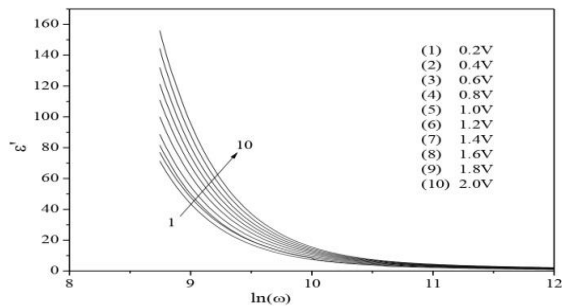


Figure 1. Frequency dependence of ϵ' for the heterojunction, Ni/n-TiO₂/p-Si/Al at different voltages

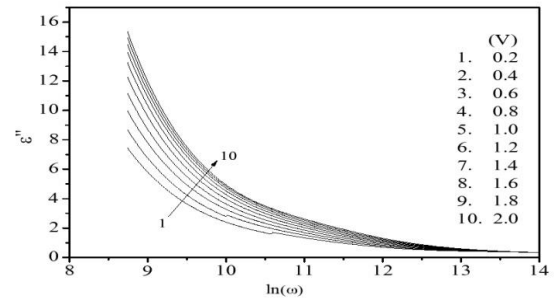


Figure 2. Frequency dependence of ϵ'' for the heterojunction, Ni/n-TiO₂/p-Si/Al at different voltages

noticed that at low frequency, the dielectric constant decreases as the frequency increases, hence showing strong dependence on the signal frequency, which is popularly known as dielectric dispersion. However, the dielectric constant increases as the temperature increases (step size 20 K). Such variations were shown by the heterojunction because the dipoles are not able to orient themselves in low temperatures regimes. However, with rise in temperature, the alignment of dipoles becomes easier (following thermal movements) which results in the increase of dielectric constant values.

Figure 4 depicts the variations of measured imaginary dielectric constant, ϵ'' of the heterojunction with respect to the frequency of the ac signal at different temperatures. With the increase in temperature the dielectric loss increases showing similar behavior as noticed for the dielectric constant in Figure 3. At high temperatures the large values of the dielectric loss, ϵ'' and sharp decrease with frequency shows the contributions of space charge polarizations and conductivity of the device. Moreover, this also clearly predicts thermally activated behavior of the dielectric relaxation process of the device. The rapid increasing behavior of ϵ'' with temperature at small frequencies may be attributed to the polarization phenomenon taking place due to the thermally activated transport mechanism of mobile charges and the defects. Large values of dielectric constants are found only either

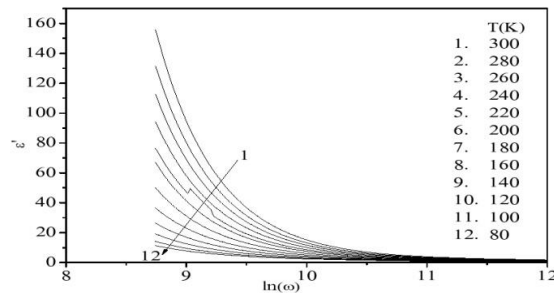


Figure 3. Frequency dependence of ϵ' for the heterojunction, Ni/n-TiO₂/p-Si/Al at different temperatures

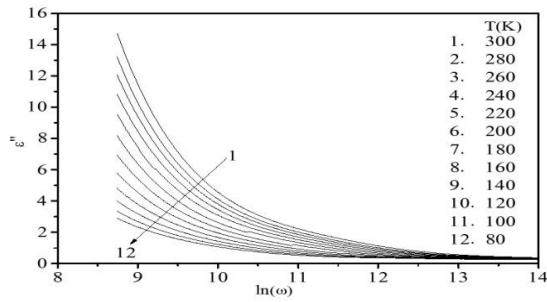


Figure 4. Frequency dependence of ϵ'' for the heterojunction, Ni/n-TiO₂/p-Si/Al at different temperatures

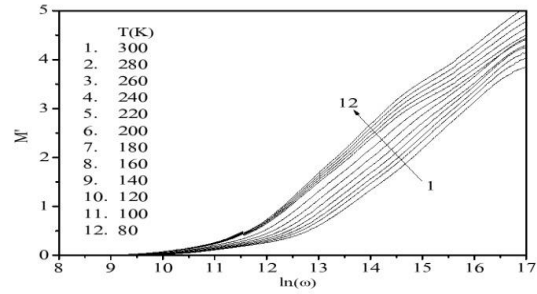


Figure 5. Frequency dependence of M' for the heterojunction, Ni/n-TiO₂/p-Si/Al at different temperatures

at low frequencies or high temperature because of the buildup of free charges at the interfaces between the sample and the electrodes called space-charge polarization process [7].

3. 3. Complex Modulus Analysis

More information can be obtained from the admittance spectroscopy data in the form of electric modulus formalisms. Variations of electric modulus with AC signal frequency allow us to confirm the existence of relaxation mechanisms in Ni/n-TiO₂/p-Si/Al heterojunction. The electric modulus analysis, real as well as the imaginary part provides significant information about electrode polarization and electrical conductivity [37]. For the considered heterostructure real and imaginary electric modulus are calculated from ϵ' and ϵ'' data as:

$$M^* = \frac{\epsilon'}{\epsilon'^2 + \epsilon''^2} + i \frac{\epsilon''}{\epsilon'^2 + \epsilon''^2} = M' + iM'' \quad (4)$$

Figure 5 depicts the variations in the real part of electric modulus with angular frequency at selected values of device temperature. The variations clearly show that M' approaches to zero at low frequencies. Moreover M' has a dispersing behavior at each temperature and at higher frequencies it tends towards M'_∞ . Monotonous increasing behavior of M' with the increasing frequency at each temperature is due to the presence of transport mechanism and very limited charge mobility under the influence of an induced electric field. These results imply the lack of restoring force which governs the mobility of the carriers. Figure 6 reports the frequency dependent variations of imaginary part of electric modulus (M'') at different selected temperatures. The M'' versus frequency plot evidently illustrates the strong thermally activated relaxation peaks whose positions i.e. M''_{max} get shifted towards high frequency region as the device temperature increases. The charge carriers being mobile at short distances are confined to potential wells at frequency above the peak maximum, whereas they are mobile at long distances in the frequency region below peak maximum. So, the frequency corresponding to the

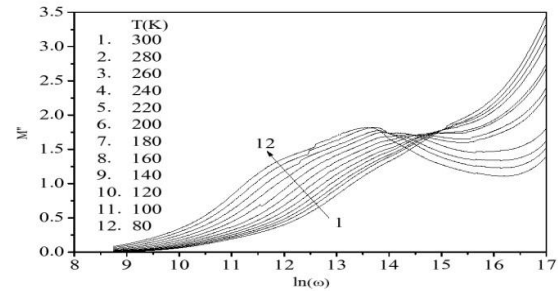


Figure 6. Frequency dependence of M'' for the heterojunction, Ni/n-TiO₂/p-Si/Al at different temperatures

peak is indicative of transition from short range to long range charge mobility. From the behavior of M'' the hopping mechanism get confirmed which intrinsically dominates in the material.

Figures 7 and 8 illustrate frequency dependent variations of logarithmic M' and M'' for the Ni/n-TiO₂/p-Si/Al heterojunction at different selected voltages. With an increase in the frequency both the parameters show increasing trends because of the polarization [42]. Corresponding to $M_\infty = 1/\epsilon'_\infty$, these parameters attain certain maximum values for each voltage at high frequencies due to relaxation processes [42-43]. At low frequencies M' and M'' almost approach to zero value. It is obvious that charge effect appears in these devices because of the release of charge from the surface states or interface traps on the application of appropriate external ac voltage [40]. Hence, the peak behavior in electric modulus indicates the existence of relaxation phenomena [44]. Due to short range charge mobility M' increases rapidly with increasing frequency and it is due to the lack of restoring force which govern the mobility of the carriers under the influence of electric field [45-47]. Correlation between the charge motions is exhibited by the imaginary part of the electric modulus [45-47]. Moreover, the conduction mechanism is dominated by the hopping of carriers between surface states i.e. the conductivity may be treated as electric field activated hopping from traps to traps.

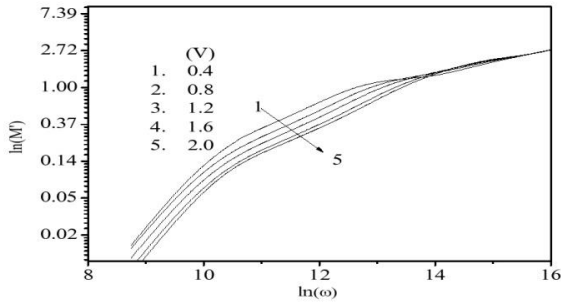


Figure 7. Frequency dependence of M' for the heterojunction, Ni/n-TiO₂/p-Si/Al at different voltages

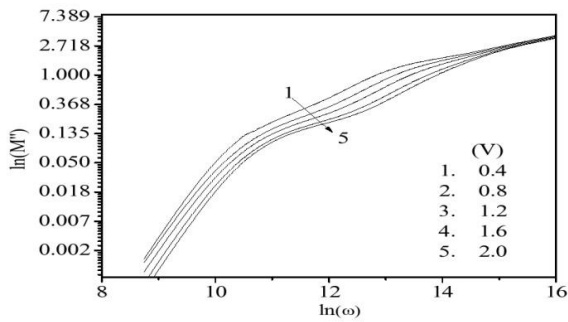


Figure 8. Frequency dependence of M'' for the heterojunction, Ni/n-TiO₂/p-Si/Al at different voltages

3. 4. Electrical Conductivity Analysis The complex conductivity σ^* obtained from the dielectric loss values can be expressed by the following relation:

$$\sigma^* = i\epsilon_0\omega\epsilon^* = i\epsilon_0\omega(\epsilon' - i\epsilon'') = \epsilon_0\omega\epsilon'' + i\epsilon_0\omega\epsilon' \quad (5)$$

The real part of σ^* is called ac conductivity (σ_{ac}) given by:

$$\sigma_{ac} = \epsilon_0\omega\epsilon'' \quad (6)$$

Figure 9 shows the dependence of the electric conductivity on the frequency at various selected temperatures. The graph reveals the conductivity dispersion which occurs due to the polarization effects in low frequency region [48]. Drop of conductivity at low frequency region occurs due the accumulation of charge. The frequency dependence of electrical conductivity is explained by Jonscher's power law given by:

$$\sigma_{ac} = \sigma_{dc} + A\omega^n \quad (7)$$

where, DC conductivity is denoted by σ_{dc} at frequency limiting to zero value, $\omega = 2\pi f$ denotes the angular frequency, A is called pre-exponential constant, and n represents the power law exponent whose value lies

between zero and one i.e. $0 < n < 1$ [49]. From the plot it is found that the conductivity of the device also increases with temperature. The dependence of AC conductivity on frequency for the heterojunction, Ni/n-TiO₂/p-Si/Al, has been obtained using the following equation [49]:

$$\sigma_{ac} = \epsilon''\omega\epsilon_0 \quad (8)$$

at different selected external applied voltages applied at room temperature and shown in Figure 10. The polarization decreases with increase in frequency which results in an increase in AC conductivity of the considered heterojunction. The higher values of AC conductivity increase the eddy currents as well as energy losses. The observed trends are found to be compatible with those quoted in literature, wherein it was recommended that the gradual decrease in series resistance (R_s) with increasing frequency increases the AC conductivity [39-40]. σ_{ac} increases with an increase in voltage as well as frequency. This is attributed to the fact that the dipoles in the heterostructure have better polarization as the increase of voltage and frequency.

The overall variations in the ϵ' , ϵ'' , M' , M'' and ac electric conductivity (σ_{ac}) are the result of reordering and restructuring of charges at the interface of Ni/n-TiO₂/p-Si/Al heterojunction under the effect of external electric field or voltage and interface polarization.

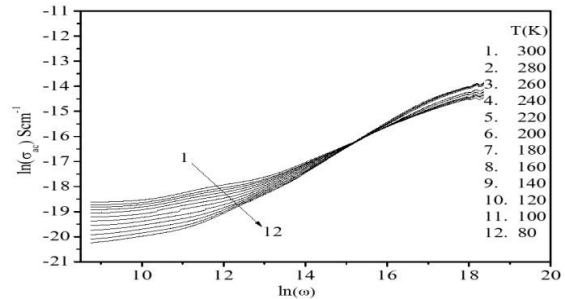


Figure 9. Frequency dependence of σ_{ac} for the heterojunction, Ni/n-TiO₂/p-Si/Al at different temperatures

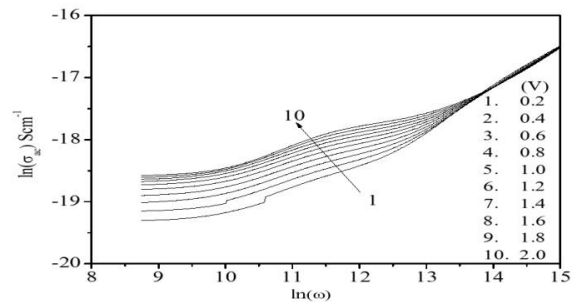


Figure 10. Frequency dependence of σ_{ac} for the heterojunction, Ni/n-TiO₂/p-Si/Al at different voltages

4. CONCLUSION

The paper reports the analysis of the dielectric properties at the interface of n-TiO₂/p-Si heterojunction obtained through pulsed laser deposition process in wide range of applied bias and temperature with frequency. The parameters ϵ' , ϵ'' , M' , M'' and AC electric conductivity (σ_{ac}) have been obtained through admittance spectroscopy ($C-V$ and $G/\omega-V$) measurements. These parameters are sensitive to applied voltage and temperature at wide range of frequency. The parameters ϵ' and ϵ'' decrease while electric moduli as well as AC conductivity increase with the frequency. The values of ϵ' , ϵ'' , σ_{ac} increase while the values of M' and M'' decrease with increase in temperature. The value of σ_{ac} increases with the increasing frequency and temperature. The increase in the σ_{ac} with the increasing temperature can be attributed to the rise in thermally generated free charge carriers. The observed behavior is due to the mobility of charge carriers in TiO₂ thin film, which are responsible for electronic polarization and hopping across the surface states. The frequency and temperature dependence of $C-V$ and $G/\omega-V$ characteristics confirmed that both the frequency and the temperature variations strongly affect the dielectric permittivity, AC conductivity and electric moduli. The findings can be inferred to suggest that interfacial polarization can occur more easily at low frequencies, thus leading to the Ni/n-TiO₂/p-Si/Al heterostructure variance of dielectric properties and electrical conductivity.

5. REFERENCES

1. Cho, M., Seo, JH., Park, DW., Zhou, W., Ma, Z., "Capacitance-voltage characteristics of Si and Ge nanomembrane based flexible metal-oxide-semiconductor devices under bending conditions", *Applied Physics Letters*, Vol. 108, (2016), 233505, <https://doi.org/10.1063/1.4953458>.
2. Pudasaini, PR., Noh, JH., Wong, AT., Ovchinnikova, OS., Haglund, AV., Dai, S., Ward, TZ., Mandrus, D., Rack, PD., "Ionic liquid activation of amorphous metal-oxide semiconductors for flexible transparent electronic devices", *Advanced Functional Materials*, Vol. 26, (2016), 2820-2825, <https://doi.org/10.1002/adfm.201505274>.
3. Kocyigit, A., Orak, I., Turut, A., "Temperature dependent dielectric properties of Au/ZnO/n-Si heterojunction", *Materials Research Express*, Vol. 5, (2018), 035906, <https://doi.org/10.1088/2053-1591/aab2e3>.
4. Sze, SM., "Physics of Semiconductor Devices, 2nd Edition, Wiley, New York", (1981).
5. Deuling, H., Klausmann, E., Goetzberger, A., "Interface states in Si/SiO₂ interfaces", *Solid State Electronics*, Vol. 15, (1972), 559-571, [https://doi.org/10.1016/0038-1101\(72\)90157-8](https://doi.org/10.1016/0038-1101(72)90157-8).
6. Kar, S., Narasimhan, RI., "Characteristics of the Si/SiO₂ interface states in thin (70-230 Å) oxide structures", *Journal of Applied Physics*, Vol. 61, (1987), 353-359, <https://doi.org/10.1063/1.338273>.
7. Dokme, I., Altindal, S., "The $C-V$ and $G/\omega-V$ characteristics of Au/SiO₂/n-Si capacitors", *Physica B*, Vol. 391, (2007), 59-64, <https://doi.org/10.1016/j.physb.2006.08.049>.
8. Yucedag, I., Altindal, S., Tataroglu, A., "On the profile of frequency dependent series resistance and dielectric constant in MIS structure", *Microelectronic Engineering*, Vol. 84, (2007), 180-186, <https://doi.org/10.1016/j.mee.2006.10.071>.
9. Kar, S., Varma, S., "Determination of silicon-silicon dioxide interface state properties from admittance measurements under illumination", *Journal of Applied Physics*, Vol. 58, (1985), 4256-4266, <https://doi.org/10.1063/1.335561>.
10. Yuksel, OF., Ocak, SB., Selcuk, AB., "High frequency characteristics of tin oxide thin films on Si", *Vacuum*, Vol. 82, (2008), 1183-1186, <https://doi.org/10.1016/j.vacuum.2008.02.002>.
11. Demirezen, S., "Frequency and voltage dependent dielectric properties and electrical conductivity of Au/PVA (Bi-doped)/n-Si Schottky barrier diodes at room temperature", *Applied Physics A*, Vol. 112, (2013), 827-833, DOI 10.1007/s00339-013-7605-7.
12. Padma, R., Lakshmi, BP., Reddy, VR., "Capacitance frequency ($C-f$) and conductance frequency ($G-f$) characteristics of Ir/n-InGaN Schottky diode as a function of temperature", *Superlattices and Microstructures*, Vol. 60, (2013), 358-369, <https://doi.org/10.1016/j.spmi.2013.05.014>.
13. Tekeli, Z., Gokcen, M., Altindal, S., Ozelcik, S., Ozbay, E., "On the profile of frequency dependent dielectric properties of (Ni/Au)/GaN/Al_{0.3}Ga_{0.7}N heterostructures", *Microelectronics Reliability*, Vol. 51, (2011), 581-586, <https://doi.org/10.1016/j.microrel.2010.09.018>.
14. Hill, W.A., Coleman, CC., "A single-frequency approximation for interface-state density determination", *Solid State Electronics*, Vol. 23, (1980), 987-993, [https://doi.org/10.1016/0038-1101\(80\)90064-7](https://doi.org/10.1016/0038-1101(80)90064-7).
15. Orak, I., Kocyigit, A., Karatas, S., "The analysis of the electrical and photovoltaic properties of Cr/p-Si structures using current-voltage measurements", *Silicon*, Vol. 10, (2018), 2109-2116, <https://doi.org/10.1007/s12633-017-9731-x>.
16. Rayssi, C., Rhouma, FIH., Dhahri, J., Khirouni, K., Zaidi, MA. Belmabrouk, H., "Structural, electric and dielectric properties of Ca_{0.85}Er_{0.1}Ti_{1-x}Co_{4x/3}O₃ (0 ≤ x ≤ 0.1)", *Applied Physics A: Materials Science and Processing*, Vol. 123, (2017), 1-13, <https://doi.org/10.1007/s00339-017-1365-8>.
17. Tataroglu, A., "Electrical and dielectric properties of MIS Schottky diodes at low temperatures", *Microelectronics Engineering*, Vol. 83, (2006), 2551-2557, <https://doi.org/10.1016/j.mee.2006.06.007>.
18. Baris, B., "Frequency dependent dielectric properties in Schottky diodes based on rubrene organic semiconductor", *Physica E*, Vol. 54, (2013), 171-176, DOI:10.1016/j.physe.2013.06.018.
19. Shiwakoti, N., Bobby, A., Asokan, K., Antony B., "Temperature dependent dielectric studies of Ni/n-GaP Schottky diodes by capacitance and conductance measurements", *Materials Science in Semiconductor Processing*, Vol. 42, (2016), 378-382, <https://doi.org/10.1016/j.mssp.2015.11.010>.
20. Schroder, DK., "Semiconductor material, device characterization, Wiley, Hoboken, NJ", (2006).
21. Symth, CP., "Dielectric behaviour and structure, McGraw-Hill, New York", (1955).
22. Fandiyeva, A., Demirezen, IM., Altindal, S., "Temperature dependence of forward and reverse bias current voltage characteristics in Al-TiW-PtSi/n-Si Schottky barrier diodes with the amorphous diffusion barrier", *Journal of Alloys and*

- Compounds*, Vol. 552, (2013), 423-429, <https://doi.org/10.1016/j.jallcom.2012.11.093>.
23. Pakma, O., Serin, N., Serin, T., Altindal, S., "Influence of frequency and bias voltage on dielectric properties and electrical conductivity of Al/TiO₂/p-Si/p+ (MOS) structures", *Journal of Physics D: Applied Physics*, Vol. 41, (2018), 215103, DOI: 10.1088/0022-3727/41/21/215103.
 24. Afandiyeva, IM., Bulbul, MM., Altindal, S., Bengi, S., "Frequency dependent dielectric properties and electrical conductivity of platinum silicide/Si contact structures with diffusion barrier", *Microelectronics Engineering*, Vol. 93, (2012), 50-55, <https://doi.org/10.1016/j.mee.2011.05.041>.
 25. Sattar, AA., Rahman SA., "Dielectric Properties of Rare Earth Substituted Cu-Zn Ferrites", *Physica Status Solidi*, Vol. 200, (2003), 415-422, DOI: 10.1002/pssa.200306663.
 26. Popescu, M., Bunget, I., "Physics solid dielectrics, Amsterdam: Elsevier", 1984.
 27. Tugluoglu, N., Karadeniz, S., Sahin, M., Safak, H., "Temperature-dependent barrier characteristics of Ag/p-SnSe Schottky diodes based on I-V-T measurements", *Semiconductor Science and Technology*, Vol. 19, (2004), 1092-1097, DOI: 10.1088/0268-1242/19/9/004.
 28. Coskun, C., Biber, M., Efeoglu, H., "Temperature dependence of current-voltage characteristics of Sn/p-GaTe Schottky diodes", *Applied Surface Science*, Vol. 211, (2003), 360-366, [https://doi.org/10.1016/S0169-4332\(03\)00267-8](https://doi.org/10.1016/S0169-4332(03)00267-8).
 29. Yakuphanoglu, F., Tugluoglu, N., Karadeniz, S., "Space charge-limited conduction in Ag/p-Si Schottky diode", *Physica B*, Vol. 392, (2007), 188-191, <https://doi.org/10.1016/j.physb.2006.11.018>.
 30. Tugluoglu, N., Karadeniz, S., "Analysis of current-voltage and capacitance-voltage characteristics of perylene-monoimide/n-Si Schottky contacts", *Current Applied Physics*, Vol. 12, (2012), 1529-1535, <https://doi.org/10.1016/j.cap.2012.04.027>.
 31. Nicollian, EH., Goetzberger, A., "The Si-SiO₂ interface-electrical properties as determined by the metal-insulator-silicon conductance technique", *Bell System Technical Journal*, Vol. 46, (1967), 1055-1133, DOI: 10.1002/j.1538-7305.1967.tb01727.x.
 32. Castagne, R., Vapaille, A., "Description of the SiO₂-Si interface properties by means of very low frequency MOS capacitance measurements", *Surface Science*, Vol. 28, (1971), 157-193, [https://doi.org/10.1016/0039-6028\(71\)90092-6](https://doi.org/10.1016/0039-6028(71)90092-6).
 33. Kumar, N., Chand, S., "Effects of temperature, bias and frequency on the dielectric properties and electrical conductivity of Ni/SiO₂/p-Si MIS Schottky diodes", *Journal of Alloys and Compounds*, Vol. 817, (2019), 153294, <https://doi.org/10.1016/j.jallcom.2019.153294>.
 34. Wagner, KW., "Zur Theorie der unvollkommenen Dielektrika", *Annals of Physics*, Vol. 40, (1913), 817-855, <https://doi.org/10.1002/andp.19133450502>.
 35. Bidault, O., Goux, P., Kchikech, M., Belkaoumi, M., Maglione, M., "Space-charge relaxation in perovskites", *Physical Review B*, Vol. 49, (1994), 7868-7873, <https://doi.org/10.1103/PhysRevB.49.7868>.
 36. Gorodea, I., Goanta, M., Toma, M., "Impact of A cation size of double perovskite A₂AlTaO₆ (A = Ca, Sr, Ba) on dielectric and catalytic properties", *Journal of Alloys Compounds*, Vol. 632, (2015), 805-809, <https://doi.org/10.1016/j.jallcom.2015.01.310>.
 37. Sutar, BC., Choudhary, RNP., Das, PR., "Dielectric and impedance spectroscopy of Sr(Bi_{0.5}Nb_{0.5})O₃ ceramics", *Ceramic International*, Vol. 40, (2014), 7791-7798, <https://doi.org/10.1016/j.ceramint.2013.12.122>.
 38. Ho, J., Jow, TC, Boggs, S., "Historical introduction to capacitor technology", *IEEE Electrical Insulation Magazine*, Vol. 26, (2010), 20-25, DOI: 10.1109/MEI.2010.5383924.
 39. Lin, JH., Zeng, JJ., Lin, YJ., "Electronic transport for graphene/n-type Si Schottky diodes with and without H₂O₂ treatment", *Thin Solid Films*, Vol. 550, (2014), 582-586, <https://doi.org/10.1016/j.tsf.2013.11.079>.
 40. Chandrakala, HN., Bommulu, R., Shivakumaraiah, Madhu, G.M., Hatna, S., "The influence of zinc oxide-cerium oxide nanoparticles on the structural characteristics and electrical properties of polyvinyl alcohol films", *Journal of Materials Science*, Vol. 47, (2012), 8076-8084, DOI: 10.1007/s10853-012-6701-y.
 41. Tataroglu, A., Altindal, S., "Study on the frequency dependence of electrical and dielectric characteristics of Au/SnO₂/n-Si (MIS) structures", *Microelectronics Engineering*, Vol. 85, (2008), 1866-1871, DOI: 10.1016/j.mee.2008.05.025.
 42. Tripathi SK., Sharma, M., "Analysis of the forward and reverse bias I-V and C-V characteristics on Al/PVA:n-PbSe polymer nanocomposites Schottky diode", *Journal of Applied Physics*, Vol. 111, (2012), 074513, <https://doi.org/10.1063/1.3698773>.
 43. Yeriskin, SA., Unal, HI., Sari, B., "Electrical and dielectric characteristics of Al/polyindole Schottky barrier diodes. II. frequency dependence", *Journal of Applied Polymer Science*, Vol. 120, (2011), 390-396, DOI: 10.1002/app.33148.
 44. Ishai, PB., Sader, E., Feldman, Y., Felner, Y., Weger, M., "Dielectric properties of Na_{0.7}CoO₂ and of the superconducting Na_{0.3}CoO₂·13H₂O", *Journal of Superconductivity*, Vol. 18, (2005), 455-459, DOI: 10.1007/s10948-005-0024-z.
 45. Pissis, P., Kyritsis, A., "Electrical conductivity studies in hydrogels", *Solid State Ionics*, 97, (1997), 105-113.
 46. Champness, CH., Clark, WR., "Anomalous inductive effect in selenium Schottky diodes", *Applied Physics Letters*, Vol. 56, (1990), 1104-1106, <https://doi.org/10.1063/1.102581>.
 47. Prabakar, K., Narayandass, SK., Mangalaraj, D., "Dielectric properties of Cd_{0.6}Zn_{0.4}Te thin films", *Physica Status Solidi*, Vol. 199, (2003), 507-514, doi.org/10.1002/pssa.200306628
 48. Du, H., Li, Y., Li, H., Shi, X., Liu, C., "Relaxor behavior of bismuth layer-structured ferroelectric ceramic with m=2", *Solid State Communications*, Vol. 148, (2008), 357-360, [10.1016/j.ssc.2008.05.017](https://doi.org/10.1016/j.ssc.2008.05.017).
 49. Dutta, P., Biswas, S., De, SK., "Dielectric Relaxation in Polyaniline-polyvinyl alcohol composites", *Materials Research Bulletin*, Vol. 37, (2002), 193-200, [https://doi.org/10.1016/S0025-5408\(01\)00813-3](https://doi.org/10.1016/S0025-5408(01)00813-3).

Persian Abstract

چکیده

در مطالعه حاضر خواص دی الکتریک مانند ثابت دی الکتریک (ϵ')، تلفات دی الکتریک (ϵ'')، بخش واقعی مدول الکتریکی (M')، قسمت خیالی مدول الکتریکی (M'') و رسانایی الکتریکی AC (σ_{ac}) در طیف وسیعی از ولتاژ اعمالی بررسی شده است. دما و فرکانس برای اتصال ناهمگون Ni/n-TiO₂/p-Si/Al. یک لایه نانوکریستالی TiO₂ بر روی سیلیکون دوپ شده با بور نوع p در محیط کنترل شده با اکسیژن با استفاده از لیزر اگزایمر بهینه شده KrF رشد داده شد. تماس اهمی فلزات نیکل خالص و آلومینیوم به ترتیب روی TiO₂ و سیلیکون با سیستم پوشش حرارتی ایجاد شد. ویژگی هایی که با کمک اندازه گیری های رسانایی-ولتاژ و ظرفیت-ولتاژ به دست می آیند که به عنوان طیف سنجی امپدانس/ادمیتانس نیز شناخته می شوند. پارامترهای مورد مطالعه به فرکانس، دما و ولتاژ بسیار حساس هستند. بازسازی و ترتیب مجدد چگالی حالت رابط به دلیل تغییرات دما و قطبش های سطحی به دلیل تغییرات فرکانس در مجموع منجر به تغییرات مشاهده شده در و . با افزایش فرکانس هدایت AC و مدول الکتریکی نیز افزایش می یابد. مکانیسم آرامش را می توان در تحلیل مدول الکتریکی پیچیده مشاهده کرد. فرآیند هدایت حرارتی فعال شده با هدایت AC وابسته به فرکانس در دماهای مختلف نشان داده شد. با استفاده از قانون توان، هدایت AC مورد تجزیه و تحلیل قرار گرفت و مشخص شد که با دما و ولتاژ اعمالی افزایش می یابد.